Supporting Information

Artemenko et al. 10.1073/pnas.1211304109

SI Materials and Methods

Cell Growth and Differentiation. *Dictyostelium discoideum* cells (Ax2 strain) were maintained under axenic conditions in HL5 medium supplemented with antibiotics. Cells carrying expression constructs were selected with either 20 μg/mL G418 or 50 μg/mL Hygromycin B as required for at least a week before analysis. For cells carrying constructs in pDM359 (1), protein expression was induced with 10 μg/mL doxycycline for 16–24 h before analysis unless otherwise specified. Developmental assays were performed as previously described using exponentially growing cells (2). Briefly, for development on a bacterial lawn, cells diluted in HL5 medium without antibiotics were plated with a suspension of *Klebsiella aerogenes* on an SM/5 plate and imaged after 4 d. For development on nonnutrient agar, cells were washed with developmental buffer (DB) [phosphate buffer (PB) supplemented with 2 mM $MgSO_4$ and 0.2 mM $CaCl_2$], plated on solidified nonnutrient DB agar, and imaged at the indicated times up to 48 h. To obtain aggregation-competent cells used in chemotaxis to cAMP and immunoblotting assays, cells were differentiated by starvation for 5 h in DB with 50 nM cAMP added every 6 min for the last 4 h.

Generation of Gene Disruptions. *krsB*$^-$ cells were generated by replacing the region between +150 and +3534, in which +1 is the first and +3723 is the last nucleotide of the *krsB* ORF, with a Blasticidin S resistance (BSR) cassette by homologous recombination. All primer sequences used in this study are shown in Table S3. The deletion construct was generated as follows: The first genomic DNA fragment was amplified by PCR with P1 and P2 primers; the BSR cassette was derived from the pLPBLP plasmid (3); the second genomic DNA fragment was amplified by PCR with P3 and P4 primers. The entire construct then was amplified by PCR with P1 and P4 primers and transformed into *D. discoideum* Ax2 cells. Transformants were selected with 10 μg/mL blasticidin S sulfate and were plated clonally onto a *K. aerogenes* lawn as described above. Single clones were screened for successful gene disruption by PCR, Southern blotting, and immunoblotting.

A second, independent *krsB*$^-$ cell line (*krsB*$^-_2$) was generated as above, except the BSR cassette was inserted between +646 and +2907 of the *krsB* gene using genomic DNA fragments amplified with P5/P6 and P7/P8 primer pairs. The entire construct was excised by BamHI/SalI, transformed into Ax2 cells, and screened for successful gene disruption using PCR and immunoblotting. Because many observations were similar in the two *krsB*$^-$ cell lines, only the first cell line is shown in the figures, except for Fig. 1*F* and Fig. S1*C*.

To generate *krsA*/*B*$^-$ cells, the BSR cassette first was removed from *krsB*$^-$ cells by transformation with a Cre recombinase expression plasmid, pDEX-NLS-Cre, and selection with 20 μg/mL G418 (3). The *krsA* gene then was disrupted in either WT Ax2 or *krsB*$^-$ cells as above using a previously described deletion construct (4) and amplified by PCR using P9 and P10 primers. *Gβ*$^-$ cells were generated in the Ax2 background by removing most of the coding sequence.

Plasmid Construction. To generate constitutively expressed KrsB constructs tagged with GFP at the C terminus, full-length *krsB* was amplified by PCR from genomic DNA using P11 and P12 primers. $KrsB_{\Delta C}$ was amplified by PCR using P11 and P13 primers. The K52R mutation was introduced into full-length KrsB or $KrsB_{\Delta C}$ using site-directed mutagenesis with P14 and its reverse-complement primers. The resulting PCR products were subcloned into PCR4Blunt-TOPO vector (Invitrogen) and confirmed by sequencing. The plasmids were digested with BamHI/XhoI, and inserts were subcloned into BglII/XhoI sites of the pKF3 vector in frame with GFP.

For doxycycline-inducible expression, the above constructs with the GFP tag were amplified by PCR with P11 and P15 primers and were subcloned into PCR4Blunt-TOPO vector. T176A and T176E mutations were introduced into KrsB-GFP in PCR4Blunt-TOPO vector by site-directed mutagenesis with P16 (for T176A) and P17 (for T176E) and their respective reverse-complement primers. All constructs were confirmed by sequencing. The KrsB-GFP constructs were digested with BamHI/XbaI and were inserted into BglII/SpeI sites of pDM359.

Full-length KrsB, tagged with GFP at the N terminus, was cloned with BamHI/SalI into pDEX-GFP-N1 (5) after amplification from genomic DNA using P18 and P19 primers. GFP-KrsA and PH_{CRAC}-GFP constructs were described previously (4, 6). RBD_{Raf}-GFP in pDM323Raf1 and GFP-$LimE_{\Delta coil}$ in pDRHyg plasmids were kindly provided by P. J. van Haastert (University of Groningen, Groningen, The Netherlands) and D. N. Robinson (Johns Hopkins University School of Medicine, Baltimore), respectively.

Chemotaxis Assays. All chemotaxis assays of aggregation-competent cells were performed as previously described (2). Briefly, for the small population assay, cells were diluted in PB and spotted next to drops of 1 μM cAMP in PB on a hydrophobic agar surface [1% (wt/vol); Difco Noble Agar (BD Biosciences) in PB]. The area closest to the cAMP drop was imaged with differential interference contrast (DIC) illumination on a Zeiss Axiovert 200 inverted microscope equipped with a 10× objective at 30-s intervals. For the micropipette assay, differentiated cells were diluted in DB, plated on a chambered coverglass (Lab-Tek, Thermo Scientific, Nunc), allowed to adhere for at least 10 min, covered with DB, and exposed to a micropipette filled with 10 μM cAMP. Where indicated, the chambered coverglass was precoated with 0.2% (wt/vol) BSA for 10 min and rinsed twice with DB before cells were plated. Cells surrounding the micropipette were imaged every 20–30 s as indicated in the figure legends. Chemotaxis speed and index and motility speed and persistence were analyzed by the Chemotaxis Quantification software (version 1.2) generously provided by P. Iglesias and Y. Xiong (Johns Hopkins University, Baltimore) as previously described (7). For under-buffer analysis (Fig. 1*F*), differentiated cells were diluted in DB and plated in a six-well tissue-culture dish. Images were acquired with phase illumination using a 20×/0.3 (micropipette assay) or 10×/0.3 (under-buffer assay) objective on a Zeiss Observer.Z1 inverted microscope. For the micropipette assay of PH_{CRAC}- and $LimE_{\Delta coil}$-expressing cells, images were acquired with a 40×/1.3 oil objective with GFP and DIC illumination. For the analysis of chemotaxis to folic acid, vegetative cells were plated on a chambered coverglass as above and exposed to a micropipette filled with 1 mM folic acid. All images were processed using ImageJ 1.43m software (National Institutes of Health).

Random Motility Assay. Vegetative cells in HL5 medium were plated on a chambered coverglass, grown overnight, and imaged with phase illumination on a Zeiss Axiovert 200 inverted microscope equipped with a 10× objective at 30-s intervals. Motility speed and persistence were derived from the Chemotaxis Quantification software (version 1.2) as described (7).

Protein Translocation to Membrane Assay. Aggregation-competent cells expressing RBD_{Raf}, PH_{CRAC}, or $LimE_{\Delta coil}$ were diluted in DB, plated on a chambered coverglass, and allowed to adhere for at least 10 min. Images were acquired with DIC and GFP illumination on a Zeiss Observer.Z1 inverted microscope equipped with a 40×/1.3 oil objective at 5-s intervals. After two frames, cAMP was added to a final concentration of 1 μM.

Phototaxis Assay. The phototaxis assay was performed as previously described (8). Briefly, slugs were transferred using a sterile inoculation loop from the edges of colonies growing on *K. aerogenes* lawns onto water agar plates. The plates were wrapped to maintain darkness except for a 2-mm-wide opening for the entry of light. Plates were incubated at 21 °C for at least 48 h. To visualize the slugs and their tracks, cells were transferred onto a nitrocellulose membrane and stained with amido black.

Adhesion Assays. All adhesion assays were performed on vegetative cells. Static images of cells in HL5 medium were acquired with phase illumination on a Zeiss Observer.Z1 inverted microscope equipped with a 20×/0.3 objective. To calculate the relative ratio of surface area to volume, cells expressing cAR1-mCherry were plated on chambered coverglass in DB, allowed to settle for at least 10 min, and imaged with a Z-step size of 150 nm using an UltraView spinning disk confocal microscope (DM 16000; PerkinElmer) equipped with a 40×/1.25–0.75 oil objective. The resulting images were analyzed with ImageJ 1.43m software using identical parameters. First, the background was subtracted from the Z-stack, and threshold was adjusted to black and white with dark background. The desired cell was outlined either using a magic wand or manually, and the area within the outline was measured. Total cell volume was calculated as the sum of the area of each slice multiplied by the height of the slice (150 nm). Interference reflection microscopy (IRM) was performed on cells seeded on a chambered coverglass in HL5 medium using a 40× oil objective on a Zeiss LSM510 META inverted microscope equipped with a 488-nm argon laser and a reflection mirror. The parameters were adjusted until the contact area with the substrate appeared black. DIC images also were acquired for each field. Raw IRM images were converted to binary images using ImageJ 1.43m, and each cell was outlined using a magic wand to measure cell area in contact with the substrate.

For the shear flow assay, cells were diluted in DB, loaded into a microfluidic device, and allowed to settle for ∼10 min. Flow was initiated at 0.6 psi and was increased by 0.1 psi every 2 min. Images were acquired with phase illumination on a Zeiss Observer.Z1 inverted microscope equipped with a 10×/0.3 objective at 30-s intervals. Cells remaining in the field before the step increase in pressure were counted manually. The rotational adhesion assay was performed as previously described (9). Briefly, 6.25×10^4 cells/cm^2 (for cells expressing KrsB constructs in the pKF3 plasmid; Fig. 3 *E* and *F*) or 1.25×10^5 cells/cm^2 (for cells expressing KrsB constructs in pDM359; Fig. 5*C*) were plated in a six-well tissue-culture plate in HL5 medium and were grown overnight. The medium was replaced with fresh HL5, and cells were allowed to recover for 1 h. The plates were placed on an orbital shaker (G-33, New Brunswick Scientific, Edison, NJ) and rotated at 150 or 100 rpm as indicated in the figure legends. Floating and adherent cells then were counted to calculate the percent of adherent cells.

Generation of KrsB Antibody. Polyclonal antibodies were generated against the unique C-terminal region of KrsB kinase. A GST-KrsB fusion protein encompassing residues 300–1106 was expressed and purified from BL21RIL cells, and the antigen–adjuvants mixture was injected into white New Zealand rabbits. Although the serum was tested for both immunoblotting and immunofluorescence applications, endogenous KrsB could be recognized only in immunoblots.

Immunoblotting. To test for expression of cAR1, cells were collected by centrifugation at the start and end of differentiation and were resuspended to a final concentration of 1×10^8 cells/mL as described previously (2). Proteins were separated on a 4–15% Tris·HCl polyacrylamide gel (Criterion; Bio-Rad), transferred to a polyvinylidene fluoride membrane, blocked with Tris-buffered saline/0.1% (vol/vol) Tween 20 with 5% (wt/vol) skim milk, and immunoblotted with a primary anti-cAR1 antibody in Tris-buffered saline/0.1% (vol/vol) Tween 20 with 5% (wt/vol) BSA, followed by HRP-conjugated anti-rabbit secondary antibody (GE Healthcare) in blocking solution. Signal was detected by chemiluminescence using ECL Western blotting detection reagent (GE Healthcare).

To test for KrsB expression throughout development, 1×10^8 WT cells were allowed to aggregate on a 9-cm dish filled with 1.5% (wt/vol) phosphate agar and were collected at the indicated time points as previously described (10). For analysis of KrsB or KrsA expression levels in various strains, vegetative cells were collected at a density of 2×10^7 cells/mL as described above for cAR1, except that the lysates were boiled for 10 min before loading on a gel. Cells (2×10^5 in Fig. S1*C* or 3×10^5 in Fig. S1*D*) were analyzed by immunoblotting using antibodies against KrsB (this study) or KrsA (4).

For phospho-KrsB immunoblotting, aggregation-competent cells were shaken at 200 rpm for 30 min in the presence of 5 mM caffeine, washed twice with cold DB, resuspended to 4×10^7 cells/mL, and kept on ice before stimulation. Cells were stimulated with 1 μM cAMP, lysed with 3× sample buffer, and boiled for 10 min. In Fig. S5*A*, B cells were resuspended to 2×10^7 cells/mL, pretreated with 100 μM LY294002 or DMSO (vehicle) for 10 min on ice (Fig. S5*B* only), and stimulated with 10 μM cAMP. For phospho-KrsB immunoblotting of vegetative cells, lysates were collected as above for cAR1 and boiled for 10 min before loading on a gel. Proteins were separated on a gel and immunoblotted as above using a primary antibody against phosphorylated Thr183 of MST1 or phosphorylated Thr410 of PKCζ (Cell Signaling). Signal was detected by chemiluminescence using ECL Plus Western blotting-detection reagent (GE Healthcare). The blot then was stripped with Restore Plus Western blot-stripping buffer (Pierce), reprobed with a primary antibody against KrsB, and detected as described above. Equal protein loading was confirmed by staining the polyvinylidene fluoride membrane with Coomassie Brilliant Blue after immunoblotting.

Immunoprecipitation. Aggregation-competent cells were shaken at 200 rpm for 30 min in the presence of 5 mM caffeine, washed twice with cold DB, resuspended to 4×10^7 cells/mL, and kept on ice before stimulation. Cells were stimulated with 10 μM cAMP and lysed with 2× lysis buffer [20 mM Hepes (pH 7.6), 1% (vol/vol) Nonidet P-40, 100 mM NaCl, 100 mM NaF, 50 mM sodium pyrophosphate, 4 mM Na_3VO_4, 2× complete EDTA-free protease inhibitor mixture (Roche)] on ice for 5 min. Lysates were centrifuged for 5 min to remove debris, and supernatants were incubated with Chromotek GFP-Trap beads at 4 °C overnight. To obtain input samples, aliquots of the supernatants were taken before immunoprecipitation and lysed with 3× sample buffer. Immunoprecipitates were washed with 1× lysis buffer, resuspended in 2× sample buffer, and immunoblotted with an antibody against GFP.

In Vitro Kinase Assay. Vegetative cells, washed and resuspended to 2×10^7 cells/mL, were subjected to immunoprecipitation as described above. Following washes with 1× lysis buffer, the beads were washed and resuspended in 50 μL kinase buffer [20 mM Hepes (pH 7.6), 10 mM $MgCl_2$]. Reaction was initiated by the addition of 5 μCi [γ-^{32}P]ATP, allowed to proceed for 5 min at 30 °C, and stopped by the addition of 25 μL 3× sample buffer. Proteins were separated by SDS/PAGE, and the gel was dried before exposure to an autoradiography film.

Statistical Analysis. When the values for different samples were matched within the experiment, either a paired two-tailed *t* test (for two samples) or repeated measures ANOVA with a Student–Newman–Keuls posttest (for multiple samples) was used. When the number of samples varied between the groups, an unpaired two-tailed *t* test was used. A *P* value <0.05 was considered significant.

1. Veltman DM, Keizer-Gunnink I, Haastert PJMV (2009) An extrachromosomal, inducible expression system for Dictyostelium discoideum. *Plasmid* 61:119–125.
2. Artemenko Y, Swaney KF, Devreotes PN (2011) Assessment of development and chemotaxis in Dictyostelium discoideum mutants. *Methods Mol Biol* 769:287–309.
3. Faix J, Kreppel L, Shaulsky G, Schleicher M, Kimmel AR (2004) A rapid and efficient method to generate multiple gene disruptions in Dictyostelium discoideum using a single selectable marker and the Cre-loxP system. *Nucleic Acids Res* 32:e143.
4. Arasada R, et al. (2006) Characterization of the Ste20-like kinase Krs1 of Dictyostelium discoideum. *Eur J Cell Biol* 85:1059–1068.
5. Rohlfs M, Arasada R, Batsios P, Janzen J, Schleicher M (2007) The Ste20-like kinase SvkA of Dictyostelium discoideum is essential for late stages of cytokinesis. *J Cell Sci* 120:4345–4354.
6. Parent CA, Blacklock BJ, Froehlich WM, Murphy DB, Devreotes PN (1998) G protein signaling events are activated at the leading edge of chemotactic cells. *Cell* 95:81–91.
7. Kamimura Y, Devreotes PN (2010) Phosphoinositide-dependent protein kinase (PDK) activity regulates phosphatidylinositol 3,4,5-trisphosphate-dependent and -independent protein kinase B activation and chemotaxis. *J Biol Chem* 285:7938–7946.
8. Darcy PK, Wilczynska Z, Fisher PR (1994) Genetic analysis of Dictyostelium slug phototaxis mutants. *Genetics* 137:977–985.
9. Fey P, Stephens S, Titus MA, Chisholm RL (2002) SadA, a novel adhesion receptor in Dictyostelium. *J Cell Biol* 159:1109–1119.
10. Dormann D, Weijer CJ (2006) Visualizing signaling and cell movement during the multicellular stages of dictyostelium development. *Methods Mol Biol* 346:297–309.

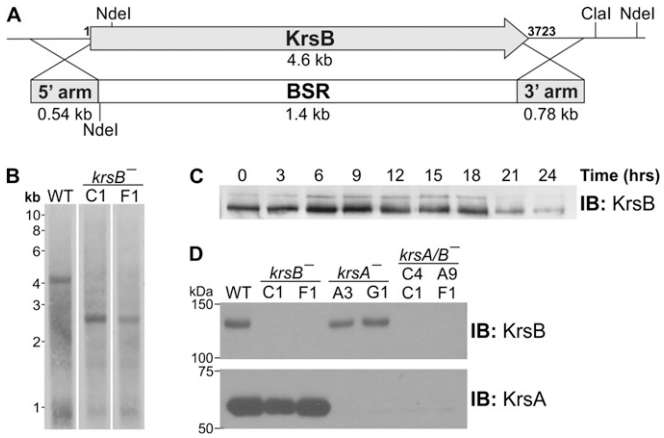

Fig. S1. Generation of *krsB*$^{-}$ cells. (*A*) Schematic of the construct used to generate *krsB*$^{-}$ cells. Crossed diagonal lines indicate the areas of homologous recombination. (*B*) Southern hybridization using a 3′-arm probe shown in *A* of genomic DNA extracted from WT and two independent clones of *krsB*$^{-}$ cell lines and digested with NdeI/ClaI. (*C*) Expression of KrsB protein visualized by immunoblotting (IB) with an antibody against KrsB during the developmental cycle. (*D*) Equal numbers of vegetative WT, *krsB*$^{-}$, *krsA*$^{-}$, and *krsA/B*$^{-}$ cells were lysed and immunoblotted with an antibody against KrsB or KrsA. Two independent clones of each null cell line are shown.

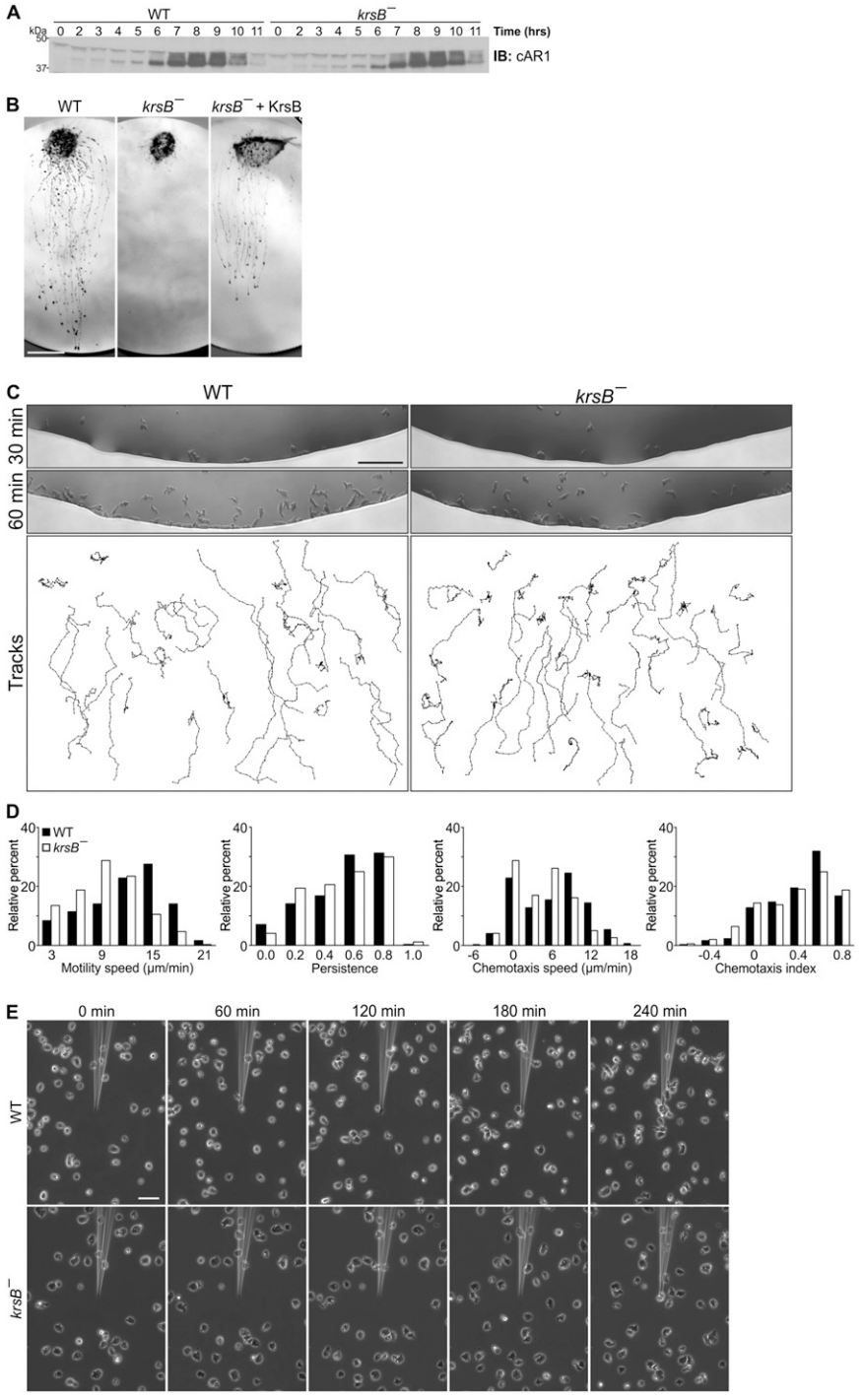

Fig. S2. KrsB is required for proper multicellular behavior and directed cell migration. (*A*) KrsB does not affect developmental marker expression. WT and *krsB*$^-$ cells were plated on nonnutrient agar at 5.2×10^5 cells/cm^2 and allowed to form fruiting bodies. At the indicated time points cells were washed off, lysed, and immunoblotted with an antibody against cAR1. (*B*) Assessment of slug phototaxis in WT, *krsB*$^-$, or *krsB*$^-$ cells expressing N-terminally GFP-tagged KrsB was performed as described in *SI Materials and Methods*. Images of the slugs transferred onto nitrocellulose membranes and stained with amido black were captured after 48 h. The light source is located at the bottom of the images. (Scale bar: 2 cm.) (*C* and *D*) Drops of aggregation-competent WT and *krsB*$^-$ cells were plated on a hydrophobic agar surface next to drops of 1 μM cAMP. DIC images were collected every 30 s from 30–60 min after the start of the assay. (*C*) Tracks of individual cells over the 30-min period (*Lower*) and snapshots (bottom edge only) (*Upper*) taken at the indicated time points are shown. The bottom edge of the drop was not included in the analysis in *D* and thus is not shown in the tracks. (Scale bar: 100 μm.) (*D*) Behavior of 298 WT and 341 *krsB*$^-$ cells obtained from six independent experiments was analyzed for various parameters using Chemotaxis Quantification Software. (*E*) Vegetative WT and *krsB*$^-$ cells plated on a chambered coverglass were exposed to a micropipette filled with 1 mM folic acid and were imaged every 30 s. Snapshots taken at the indicated time points are shown. (Scale bar: 50 μm.)

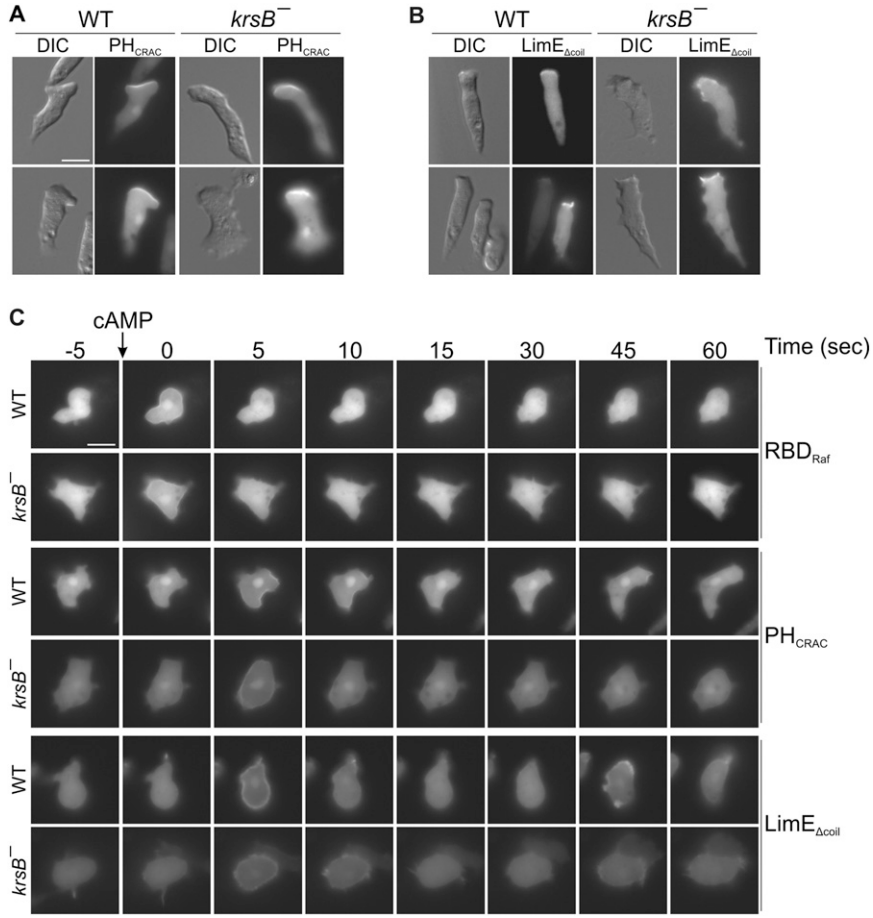

Fig. S3. Localization of leading-edge markers is not perturbed in the absence of KrsB. Analysis was performed on aggregation-competent WT and *krsB*$^{-}$ cells expressing the PH domain from CRAC (*A* and *C*), a fragment of actin-binding protein LimE (*B* and *C*), or Ras-binding domain from Raf (*C*). (*A* and *B*) Cells were plated in glass-bottomed chambers and exposed to a micropipette filled with 10 μM cAMP. DIC and fluorescence images were collected every 30 s. Two representative cells polarized in the direction of the gradient are shown for each condition. (*C*) Cells were plated in glass-bottomed chambers and globally stimulated with 1 μM cAMP. DIC and fluorescence images were acquired at 5-s intervals. A representative cell is shown for each condition. (Scale bar: 10 μm.)

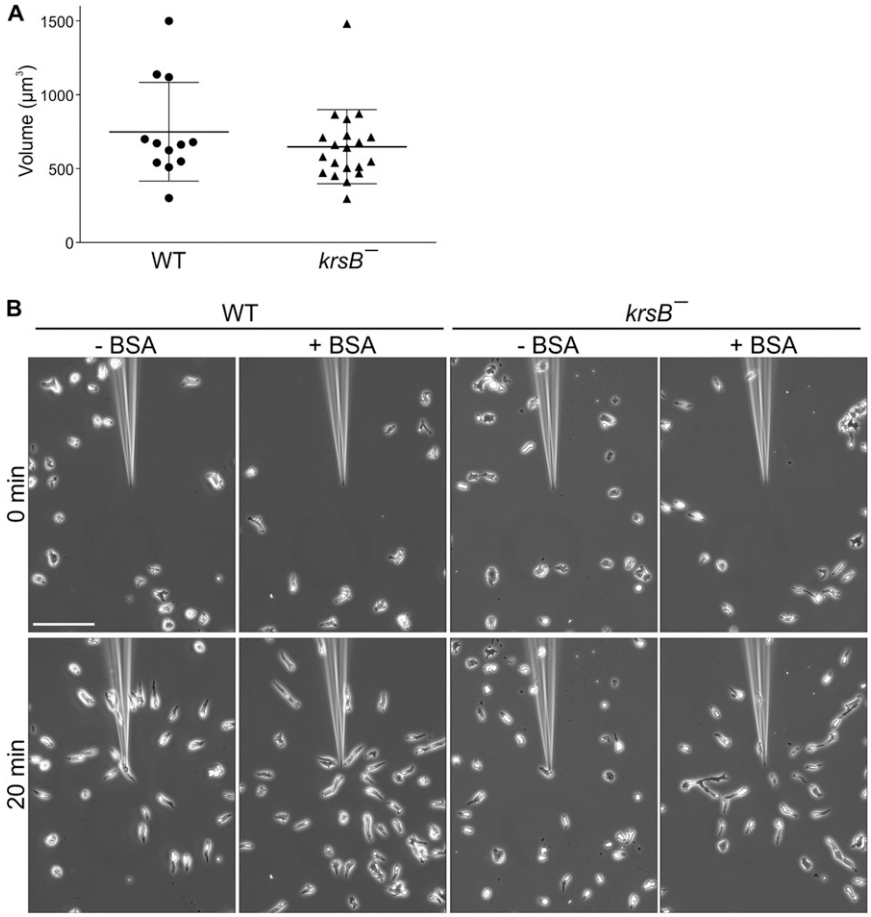

Fig. S4. Increased spreading and adhesion of *krsB*$^{-}$ cells is not caused by a change in the total volume of the cells and is responsible for their defective chemotaxis. (*A*) Vegetative WT and *krsB*$^{-}$ cells were plated in glass-bottomed chambers in phosphate buffer. Z-stacks of cAR1-mCherry were acquired with a spinning disk confocal microscope. The area of each slice from 12 WT and 20 *krsB*$^{-}$ cells was measured to derive the total volume as described in *SI Materials and Methods*. Data are shown as mean ± SD. (*B*) Aggregation-competent cells plated in glass-bottomed chambers with or without 0.2% BSA coating were exposed to a micropipette filled with 10 μM cAMP and were imaged every 15 s for 20 min. Snapshots taken at the indicated time points are shown. Tracks of individual cells over the 20-min period are shown in Fig. 3*F*. (Scale bar: 100 μm.)

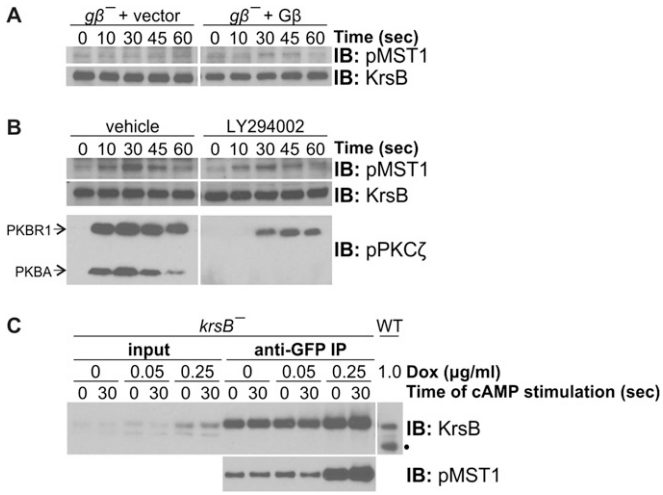

Fig. S5. Chemoattractant-stimulated phosphorylation of endogenous but of not GFP-tagged KrsB is dependent on heterotrimeric G proteins and is independent of PI3K and TorC2. (*A*) Aggregation-competent *gβ*⁻ cells expressing Gβ or empty vector were treated with 10 μM cAMP, lysed at the indicated times, and immunoblotted with an antibody against MST1 phosphorylated on Thr183 (pMST1) or KrsB. (*B*) Aggregation-competent WT cells were pretreated with 100 μM LY294002 or vehicle for 10 min and then were stimulated and immunoblotted as in *A*. To detect phosphorylation of PKBR1 and PKBA, lysates also were immunoblotted with an antibody against PKCζ phosphorylated on Thr410. Results in *A* and *B* are representative of two independent experiments, each performed in duplicate. (*C*) WT and *krsB*⁻ cells expressing C-terminally GFP-tagged KrsB under the control of a doxycycline-inducible promoter were treated with the indicated concentrations of doxycycline overnight. Aggregation-competent *krsB*⁻ cells expressing KrsB were stimulated with 10 μM cAMP, immunoprecipitated with an antibody against GFP, and immunoblotted as in *A*. Equal numbers of cells were loaded in WT and input lanes to show that the amount of KrsB-GFP in *krsB*⁻ cells before immunoprecipitation is below endogenous levels. The black circle indicates the position of the endogenous KrsB band.

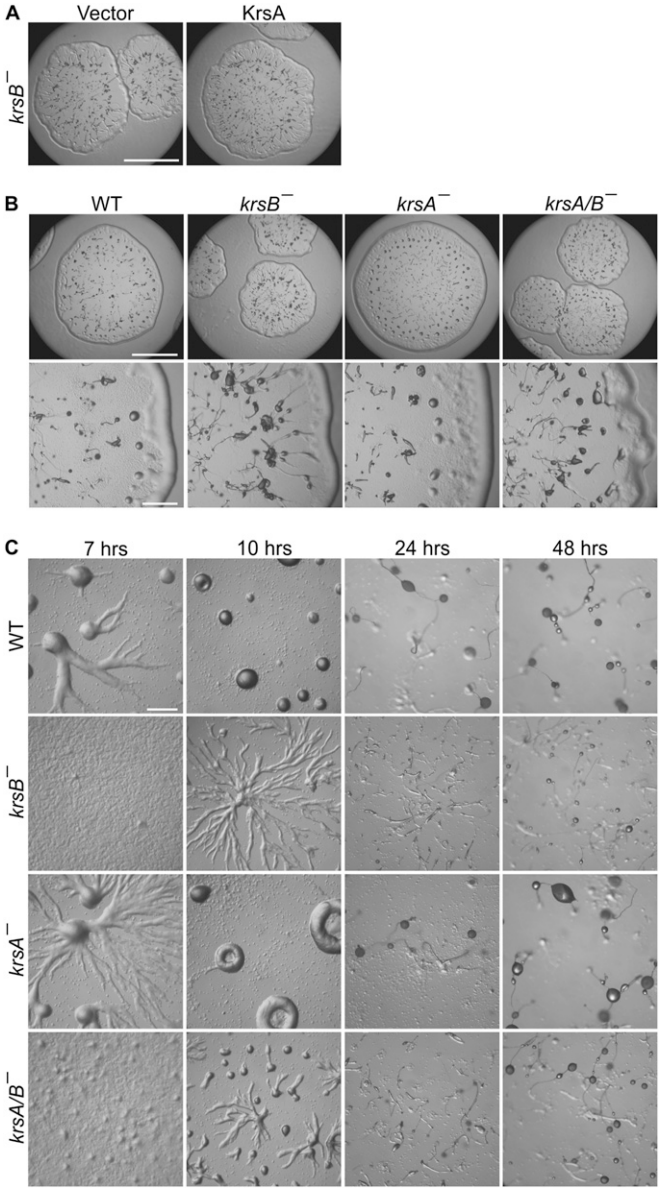

Fig. S6. KrsB is not functionally redundant with KrsA. (*A*) *krsB*$^{-}$ cells expressing empty vector or N-terminally GFP-tagged KrsA were plated on a *K. aerogenes* lawn on agar plates, and the resulting plaques were imaged after 4 d. (Scale bar: 5 mm.) (*B*) WT, *krsB*$^{-}$, *krsA*$^{-}$, and *krsA/B*$^{-}$ cells were plated on a *K. aerogenes* lawn on agar plates, and the resulting plaques were imaged after 4 d. [Scale bars: 5 mm (*Upper*); 1 mm (*Lower*)]. (*C*) The cell lines in *B* were plated on nonnutrient agar at 5.2×10^5 cells/cm^2 and allowed to form fruiting bodies. Images were acquired at the indicated time points. (Scale bar: 0.5 mm.)

Table S1. Chemotaxis parameters for WT and *krsB*$^-$ cells in micropipette, small population, and random migration assays

	Micropipette assay[†]		Small population assay[‡]		Random migration[§]	
Parameter	WT	*krsB*$^-$	Wild type	*krsB*$^-$	WT	*krsB*$^-$
Motility speed (μm/min)	5.9 ± 0.2	5.6 ± 0.4	12.1 ± 0.7	9.4 ± 0.8*	4.8 ± 0.2	3.4 ± 0.3*
Chemotaxis speed (μm/min)	2.5 ± 0.4	1.1 ± 0.2*	6.3 ± 0.7	4.4 ± 0.7	N/A	N/A
Chemotaxis index	0.46 ± 0.07	0.18 ± 0.03*	0.43 ± 0.04	0.37 ± 0.06	N/A	N/A
Persistence	0.51 ± 0.04	0.29 ± 0.03**	0.54 ± 0.03	0.51 ± 0.04	0.33 ± 0.04	0.27 ± 0.01

N/A, not applicable
[†]Values are shown as mean ± SE; n = 3 independent experiments with 20–40 cells per experiment.
[‡]Values are shown as mean ± SE; n = 6 independent experiments with 38–78 cells per experiment.
[§]Values are shown as mean ± SE; n = 3 independent experiments with 95–255 cells per experiment.
*P < 0.05, **P < 0.01 compared with WT; analysis was done by a paired, two-tailed t test.

Table S2. Chemotaxis parameters for WT and *krsB*$^-$ cells in a micropipette assay performed on a glass surface with or without a 0.2% BSA coating

	WT		*krsB*$^-$	
Parameter	− BSA	+ BSA	− BSA	+ BSA
Motility speed (μm/min)	7.2 ± 0.3[†]	12.2 ± 1.9*	6.4 ± 0.5	10.9 ± 1.3*
Chemotaxis speed (μm/min)	2.9 ± 0.6	8.4 ± 1.5*	0.72 ± 0.27	6.2 ± 1.2*
Chemotaxis index	0.41 ± 0.10	0.61 ± 0.08	0.13 ± 0.04[#]	0.53 ± 0.06*
Persistence	0.50 ± 0.07	0.76 ± 0.05*	0.29 ± 0.04[#]	0.70 ± 0.05**

[†]Mean ± SE; n = 3 independent experiments with 26–59 cells per experiment.
*P < 0.05; **P < 0.01 compared with the condition without BSA for the same cell line; [#]P < 0.05 compared with WT cells with the same BSA treatment; analysis done by a repeated measures ANOVA with a Student–Newman–Keuls posttest.

Table S3. Primer sequences used in this study

Name	Sequence	Construct
P1	CGCGTCGACCTATTAATACAGGATAGGATCAACATCAC	*krsB*$^-$
P2	GCGCCCGGGGCGACAATGTTACCTGTCTTTTTATAAG	*krsB*$^-$
P3	CGCCCCGGGCAAGATGGTACACTAAGAGAATTTGTTT	*krsB*$^-$
P4	CGCGCGGCCGCCTCACTCTTTGGTACATTAGTC	*krsB*$^-$
P5	GTCGACATGAAGAACAAATTGCATTAGTAT	*krsB*$^-_2$
P6	GCGTCGACAAGCTTAATCAACTGAAACACCAGATTG	*krsB*$^-_2$
P7	AAAACTGCAGCCAACAATGCAATCATCAACAAC	*krsB*$^-_2$
P8	CGCGGATCCATCCAATTTATAGATTGAACCTTG	*krsB*$^-_2$
P9	CCCATCGATGAGAAATTGGGTGAAGGTTCATATGGTTC	*krsA*$^-$
P10	CGCGGATCCGATTTCTTTTCATCAATTAA	*krsA*$^-$
P11	GCAACCGGATCCAAAATAAAAATGGAGGAAAGTGGTCAACTTAGTGATTT	KrsB-GFP, KrsBΔC-GFP
P12	CACACCACCACTCGAGCCATTATTATAAAAATCTAAATCAAATTCTGAATAAATTG	KrsB-GFP
P13	CATACTCGAGCCGTAAACTGACGGTGACATTGGTAATGG	KrsBΔC-GFP
P14	AAAAGACAGGTAACATTGTCGCTGTACGATTAGTACCAATCAATGAAGATTTTC	KrsBK52R-GFP
P15	CTCCTCTAGAGTGGTACCTCTAGCAGATCC	KrsB-GFP
P16	CGTACCAGAAAGAGAAATGCGGTTATTGGTACACCATTC	KrsBT176A-GFP
P17	CGTACCAGAAAGAGAAATGAGGTTATTGGTACACCATTC	KrsBT176E-GFP
P18	GGATCCTGGAGGAAAGTGGTC	GFP-KrsB
P19	GTCGACTTAATTATTATAAAAATCTAAATCAAATTCTG	GFP-KrsB

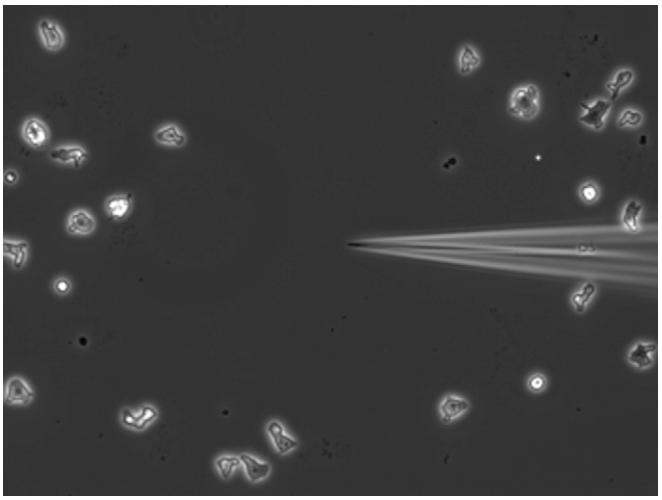

Movie S1. Migration of aggregation-competent WT cells in the presence of a micropipette filled with 10 μM cAMP. Images were captured at 30-s intervals for 30 min. Playback speed is seven frames/s. The video corresponds to Fig. 2*A*.

Movie S1

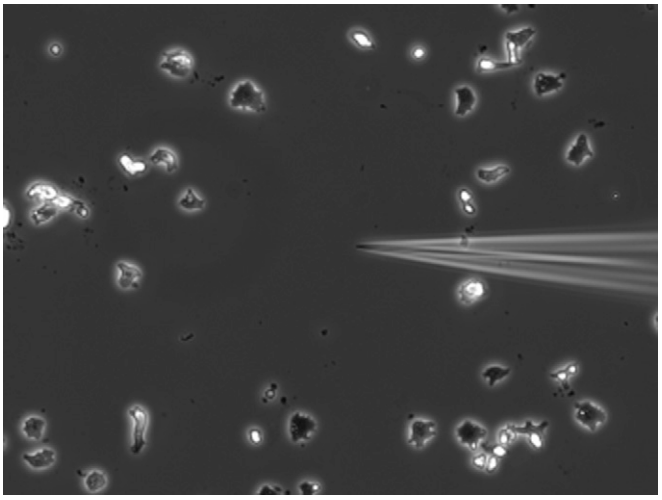

Movie S2. Migration of aggregation-competent *krsB*$^{-}$ cells in the presence of a micropipette filled with 10 μM cAMP. Images were captured at 30-s intervals for 30 min. Playback speed is seven frames/s. The video corresponds to Fig. 2*A*.

Movie S2

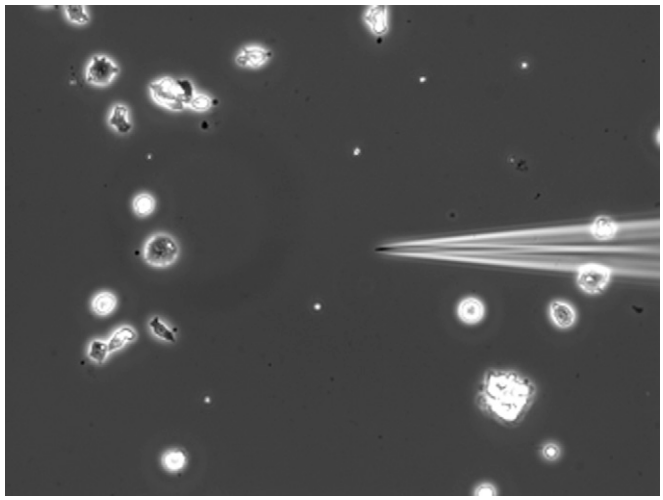

Movie S3. Migration of aggregation-competent *krsB*$^{-}$ cells expressing empty vector in the presence of a micropipette filled with 10 μM cAMP. Images were captured at 30-s intervals for 30 min. seven frames/s. The video corresponds to Fig. 2*C*.

Movie S3

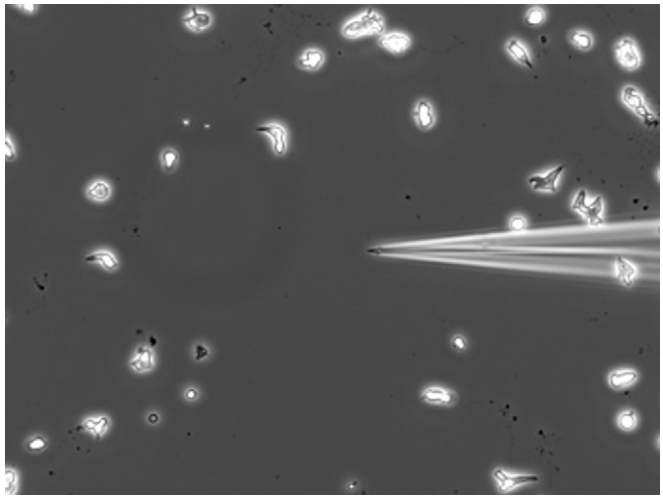

Movie S4. Migration of aggregation-competent *krsB*$^{-}$ cells expressing full-length KrsB, tagged with GFP at the C terminus in the presence of a micropipette filled with 10 μM cAMP. Images were captured at 30-s intervals for 30 min. Playback speed is seven frames/s. The video corresponds to Fig. 2*C*.

Movie S4

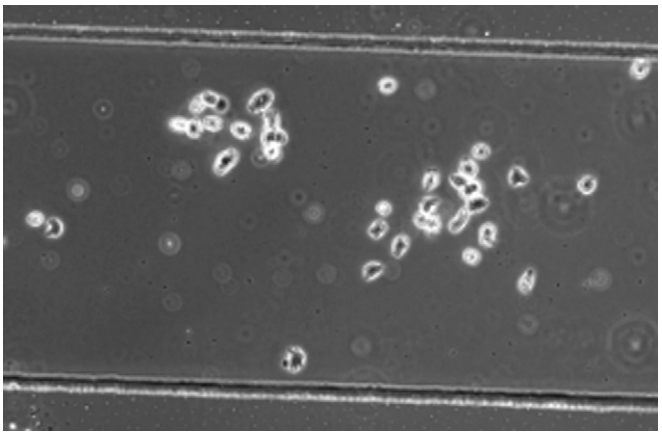

Movie S5. Response of vegetative WT cells to increasing flow in a microfluidic device. Images were captured at 30-s intervals for 55 min. Playback speed is seven frames/s. The video corresponds to Fig. 3*C*.

Movie S5

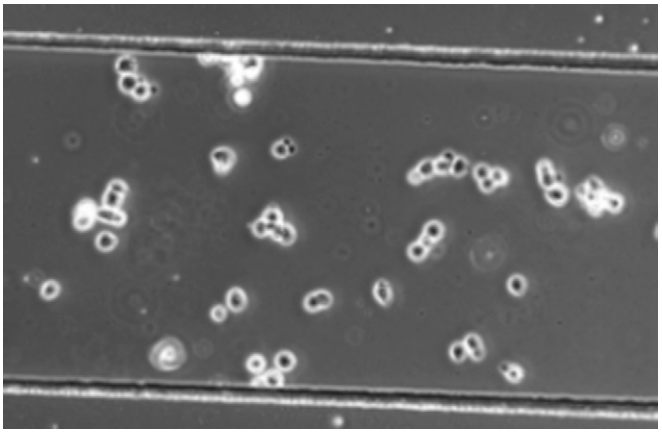

Movie S6. Response of vegetative *krsB*$^{-}$ cells to increasing flow in a microfluidic device. Images were captured at 30-s intervals for 95 min. Playback speed is seven frames/s. The video corresponds to Fig. 3*C*.

Movie S6